Room Temperature Characterization of MEMS Devices: Effects of Nearby Solid Boundary

Lucas Wilkins
University of Florida

2017-08-03

Abstract

Micro-electro-mechanical-systems (MEMS) are common devices used in consumer technologies and scientific research. MEMS devices are implemented to study quantum fluids by analyzing their mechanical resonance when submersed in fluid. Fundamental equations that describe these devices provide significant information, allowing for quantitative analysis of the oscillators' resonance. In this study, the effects of damping on the harmonic oscillators are reviewed. Comparisons are made between MEMS devices with and without a substrate. These comparisons are made by varying the pressure of N_2 gas and examining the resulting resonance frequencies. Examination of the results suggests that a damped harmonic oscillator without a close boundary experiences a changing rate of damping with pressure and that an oscillator with a close boundary experiences a linear relationship between damping and pressure when submersed in a classical fluid.

Introduction

Micro-electro-mechanical-systems (MEMS) are useful devices that appear in mobile devices, medical equipment, and even fundamental research. Specifically, in the Lee Group at University of Florida, these devices are implemented to study properties in quantum fluids at sub-millikelvin temperatures. A MEMS device is an instrument that has micro-meter length scales and is basically an electro-mechanical transducer. Their small size allows experimental equipment to house them in very small spaces, such as an ultra-low temperature cryostat. Furthermore, MEMS devices have reduced length scales [1]. Damping from a fluid scales relative to the surface area, ℓ^2, where ℓ is the characteristic length of the device. The mass of the oscillator scales with ℓ^3. Therefore, the energy ratio between the damping and its mass scales as l^{-1}, resulting in very pronounced damping effects for small devices.

The MEMS devices used in these experiments are oscillators with driving capacitors. Two variations of the oscillators are used in this work. The first variation suspends an oscillating plate over a solid substrate with a fixed gap. The second variation does not have a limiting substrate under the suspended plate. When submersed in a fluid, the devices experience a damping force. The damping upon the two versions of devices is expected to cause them to have different resonance frequencies and damping. A small gap for a fluid against an oscillating plate will cause a greater damping force than a device without a backing substrate.

To study quantum fluids with MEMS devices, it is essential to first test and fully characterize the devices in classical fluids at room temperature. Testing classical materials reveals the properties and behavior of the MEMS devices so that certain effects in later experiments with quantum fluids can be distinguished between the fluids and the devices used. In this work, the MEMS devices were tested while submerged in air and N_2 at room temperature. The goal of this study was to compare the effects of damping on the MEMS devices with and without a backing substrate. Specifically, the resonance and damping of the oscillator were measured while varying the pressure of the ambient gas pressure from 1 bar to high vacuum. The results indicate that the rate of damping changes with pressure for a MEMS device without a substrate and that the relationship between pressure and damping has a linear relationship for a device with a substrate.

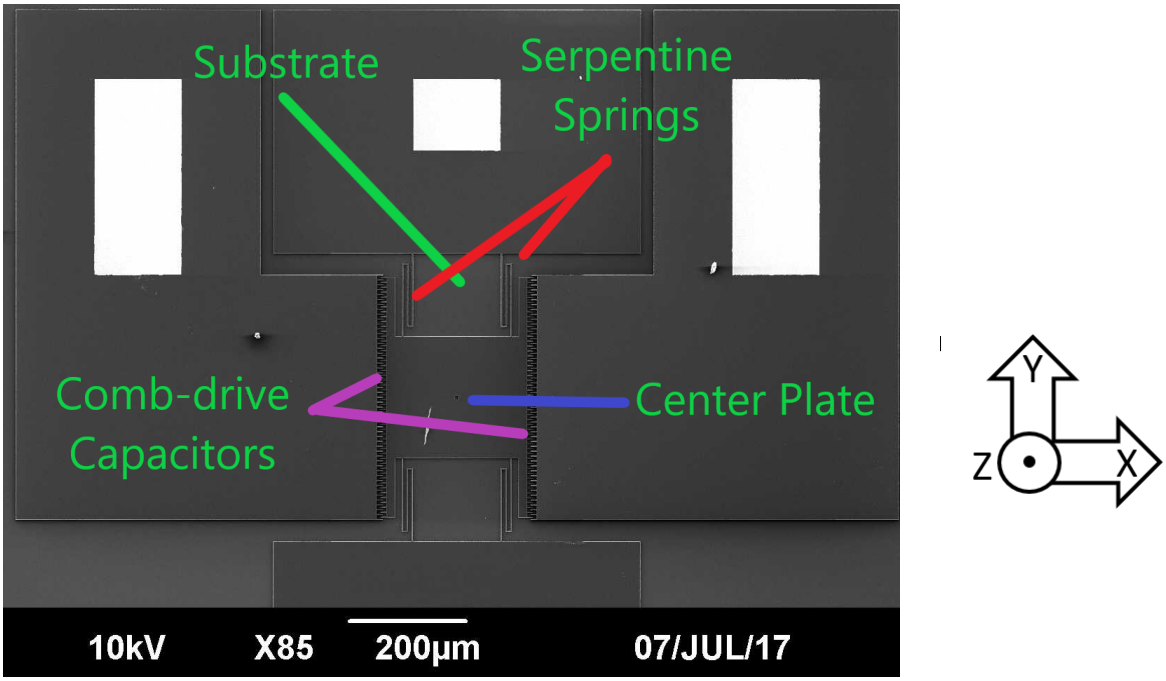

Figure 1: SEM image of MEMS device with a substrate. The center plate is located in between the comb-like capacitors. The white rectangles are gold plates that allow wire connection. Other white specs are dust particles.

MEMS Device

The MEMS devices used in this work are the third-generation design produced by the Lee Group at the University of Florida (see Fig. 1). These differ from previous generations because they contain only three layers. The bottom layer, also called the *handle* layer, is composed of Si doped with boron (4.60 μm thick). Doping a semiconductor with boron makes it conductive. The middle *sacrificial* layer of SiO_2 is 1.0 μm thick. This layer can be chemically etched to make the active elements mobile through a process called releasing. The top layer (3.0 μm thick), again composed of Si doped with boron, is patterned to form the movable components, an *active* layer. The oscillators contain a $200 \times 200\mu$m plate suspended by four serpentine springs as shown in Fig. 1. The springs allow displacements in three dimensions. The device with a substrate, contains a 1.0 μm gap that forms between the

plate and the substrate. Two comb-shaped electrodes are attached to the plate, where one faces the +x direction and the other faces the -x direction; they move with the oscillating plate. The electrodes are interwoven with fixed electrodes that are anchored to the substrate.

Each device has four possible oscillation modes with distinct resonance frequencies. These modes include the trampoline, x-pivot, y-pivot, and shear [3]. The trampoline mode involves oscillation along the z-axis. X-pivot and y-pivot are torsional oscillation modes around the x-axis and y-axis. The oscillation mode of main interest is the shear mode. It is also referred to as the *x-displacement* mode, simply because all movement is negligible except for the reciprocation of the oscillator along the x-axis [1]. This is beneficial because a constant gap is maintained for the fluid to reside and the damping is limited to one axis. The shear mode is a one-dimensional damped harmonic oscillator that can be described by three forces:

1. Restoring force by Hooke's Law: $F = -kx$
2. Damping force is proportional to the velocity of the device: $F_d = -\gamma\dot{x}$
3. Driving force from the electrode capacitors: $F_e = F_0 e^{i\omega t}$

These components work together in a system to describe the oscillator's motion modeled by a driven damped harmonic oscillator:

$$m\ddot{x} + \gamma\dot{x} + kx = F_0 e^{i\omega t}. \tag{1}$$

Given that the device is a harmonic oscillator, $x = Ae^{i\omega t}$ considers the displacement with an amplitude affected by time. The amplitude of oscillation has real and imaginary components, where the real component is in-phase and the imaginary component is out-of-phase with the real component by $\frac{\pi}{2}$. The following expressions describe the amplitude:

$$A_i(F_0, \omega) = \frac{F_0}{m} \frac{\omega_0^2 - \omega^2}{(\omega_0^2 - \omega^2)^2 + \omega^2\gamma_n^2}, \tag{2}$$

$$A_o(F_0, \omega) = \frac{F_0}{m} \frac{\omega\gamma_n}{(\omega_0^2 - \omega^2)^2 + \omega^2\gamma_n^2}, \tag{3}$$

where A_i is the in-phase component and A_o describes the out-of-phase component of the amplitude. A_i is also referred to as the *absorption* and A_o

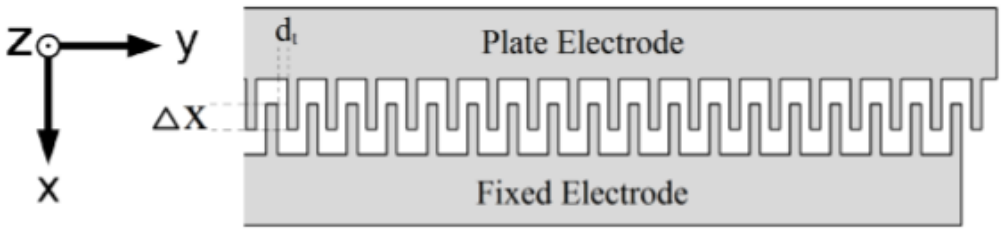

Figure 2: Capacitance electrodes. In the shear mode, the electrode attached to the plate will move along the x-axis [1].

is referred to as *dispersion*. m is the effective mass of the oscillator, ω_0 is the undamped resonance frequency ($\omega_0 = \sqrt{\frac{k}{m}}$), ω is the driving frequency, and γ_n is the damping coefficient per unit mass ($\gamma_n = \frac{\gamma}{m}$). The resonance frequency is of high interest. At resonance, the amplitude of oscillation will be the maximum.

Driving the device into oscillation utilizes comb-like capacitors called comb-drive electrodes. The total capacitance is dependent on the number of teeth pairings (N), permittivity of the fluid (ϵ), permittivity of free space (ϵ_0), thickness of the electrodes (t), gap between the teeth (d_t), and their overlap (Δx):

$$C = \frac{N\epsilon\epsilon_0 t}{d_t}\Delta x = \beta\Delta x, \tag{4}$$

where β is referred to as the *transduction* factor; it relates the electrical and mechanical properties of the device [4]. A high transduction factor results in a large capacitance, and therefore, a high driving force.

When an alternating current is applied across the electrodes, the charge on the capacitors fluctuates. Due to Coulomb's Law, $Q = CV$, where Q is proportional to V. The energy in the capacitors is: $E_C = \frac{1}{2}CV^2$. A changing V results in a change in the capacitor's energy. The change in energy induces a force on the capacitor ($F = -\frac{dE_C}{dx}$). Thus, the force on the electrodes can be calculated:

$$F = \frac{1}{2}\beta V^2. \tag{5}$$

Likewise, the velocity of the oscillator is dependent on the force between the electrodes (see Fig. 6)[4]. Therefore, the velocity can be calculated using the transduction factor since the velocity is dependent on the driving force.

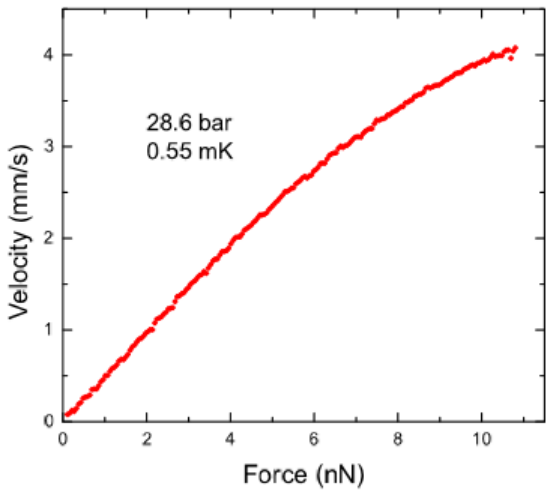

Figure 3: Velocity vs. Force calculated using the transduction factor. The velocity is dependent on the force [4].

Measurement

Driving the MEMS device is not possible without applying an AC voltage that allows for controlled fluctuations in charge. This experiment employs a symmetric "push-pull" bridge circuit, shown in Fig. 4. This setup is beneficial because it separates the coupling between voltage sources, enabling a large driving force [4]. "One-side pull" circuits can overload with high excitations due to the drastic imbalance in capacitance between the electrodes. This overload is caused by sticking and leaking from the electrodes due to an extraordinary imbalance in charge.

In the "push-pull" circuit, a high frequency carrier signal V_{HF} of $150kHz$ is first floated through an isolation transformer and split into equal and out-of-phase components (left and right) by a ratio transformer. Out-of-phase signals create the imbalance in charge on the MEMS device, allowing

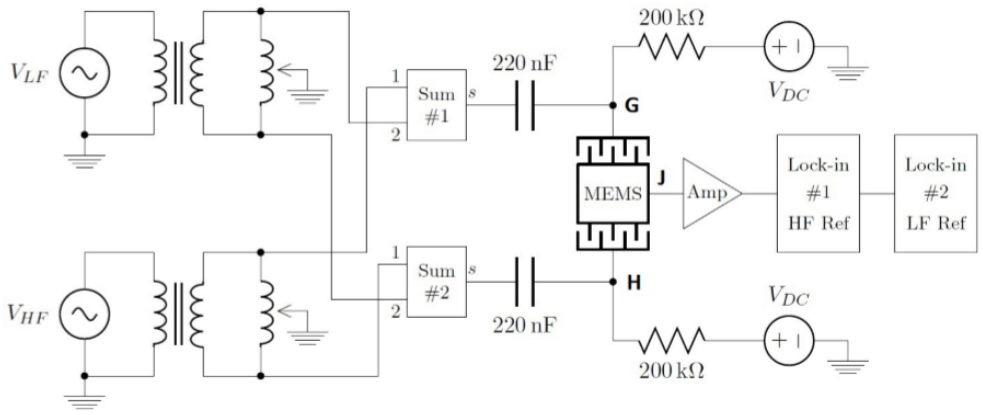

Figure 4: Diagram of the "push-pull" circuit [4]. This design allows for high excitations due to simultaneous driving forces on the left and right side of the MEMS device.

it to oscillate. Transformers significantly reduce noise in the circuit versus a schematic with a direct connection between the voltage sources and the MEMS device [4]. V_{HF} carries a low frequency signal V_{LF}, which is supplied through another isolation and ratio transformer. The left and right V_{HF} and V_{LF} signals are combined at their own signal combiners. The combined signals then flow through DC blocking capacitors of $200nF$. The signals can pass through the capacitors with little interference due to the low impedance from V_{HF}. Without the blocking capacitors, DC voltage would flow to the transformers and magnetize the inner cores, rendering them useless. A DC bias V_{DC} is supplied at $5V$ and is fed into the MEMS device along with V_{HF} and V_{LF}. A charge sensitive preamplifier converts the charge on the device to a voltage V_{out}. The signal passes through two lock-in amplifiers. The first lock-in amplifier demodulates V_{HF} and the second amplifier detects the amplitude of the oscillator created by V_{LF} [3].

Because the signals are split by ratio transformers, the force on the MEMS device is split between the left and right side:

$$F_{L,R} = \frac{1}{2}\beta(V_{DC}^2 \pm V_{DC}V_{LF} + \frac{1}{4}V_{LF}^2). \tag{6}$$

The total force on either side of the circuit is dependent on the square of V_{DC} and V_{LF} and the transduction factor.

Damping

All formulae regarding fluid flow are derived from the Navier-Stokes equation:

$$\rho[\frac{\partial u}{\partial t} + (u\dot{\nabla})u] = F - \nabla P + \eta\nabla^2 u. \tag{7}$$

The damping force F_d is provided by the viscosity of the fluid. In an ideal fluid, the velocity of the fluid matches the velocity of the moving plate and has zero relative velocity at the boundary [1]. When the MEMS plate moves, momentum is transferred through the fluid. The transfer of momentum between the particles causes resistance.

Fluid flow in the chamber depends on the version of the MEMS device. Without a substrate, the fluid velocity decreases exponentially with distance from the plate: $\nu(z) = \nu_0 e^{-\frac{z}{\delta}}$. A boundary close to the oscillating plate affects the velocity of the fluid more rapidly, and can be represented as $\nu(z) = \nu_0(1 - \frac{z}{d})$ (see Fig. 5, a).

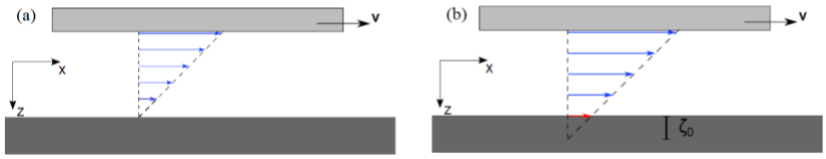

Figure 5: Illustration of fluid damping. (a) represents a situation where the velocity of the fluid matches the relative velocity of both the oscillating plate and substrate. (b) illustrates a slip length ζ that is greater than the gap between the moving plate and substrate. This causes the fluid to slip along the surfaces because the fluid's velocity can no longer match the velocity of them. This phenomenon is called *slide-film damping*.

Recall Eq. 2. F_d is dependent on the damping coefficient γ_n, and

$$\gamma_n = \frac{A}{d}(\frac{\eta}{1 + 2K_n}), \tag{8}$$

where A is the area of the plate affected by damping, d is the gap where the fluid resides, η is the fluid's viscosity, and K_n is the Knudsen number. $K_n = \frac{\lambda}{d}$, where λ is the mean free path of the fluid.

Consider a MEMS device without a substrate. In this situation, $d >> \ell$, where ℓ is the length of the device. Although there is not a substrate, the fluid will have zero velocity at some distance from the moving plate. This is called the *viscous penetration depth* δ, and can be calculated as follows:

$$\delta = \sqrt{\frac{2\eta}{\rho\omega}} \tag{9}$$

When $d >> \ell$, substitute $d = \delta$ to refine Eq. 8: $\gamma_n = \frac{A}{\delta}(\frac{\eta}{1+2K_n})$. Because pressure P is proportional to fluid density ρ, δ is inversely proportional to $\sqrt{P}$. Therefore, γ_n is proportional to $\sqrt{P}$.

A substrate under the oscillator creates the situation where $d << \ell$. The boundary is within the penetration depth of the fluid. Because the fluid will slide along the surfaces, a *slip length* ζ can be considered, which describes the theoretical distance that the fluid's velocity becomes zero if the boundary gap were extended (see Fig. 5, b) [1]. ζ is approximately equal to λ. In this situation, Eq. 8 is used without substitution to express the damping coefficient.

Experimental Methodology

MEMS devices are released using a photolithography process. A chip with eight oscillators is mounted to a socket, where the MEMS electrodes are wire bonded to the socket's connectors. Four of the devices have a substrate. One device without a substrate is connected to the circuit, and is sealed in a vacuum chamber. A TEGAM 2725A waveform generator supplies V_{HF} with a frequency of $150Hz$ and a voltage of $1V$. An Agilent 33220A waveform generator supplies V_{LF} and is modulated by the LabVIEW 2009 program. A Signal Recovery 7124 precision lock-in amplifier supplies $V_{DC} = 5V$ and also serves as the second lock-in amplifier. V_{LF} is first swept with a range of $40,000Hz$ at 1 bar to identify all resonance peaks. Smaller frequency sweeps are conducted around specific resonance peaks. For the shear mode,

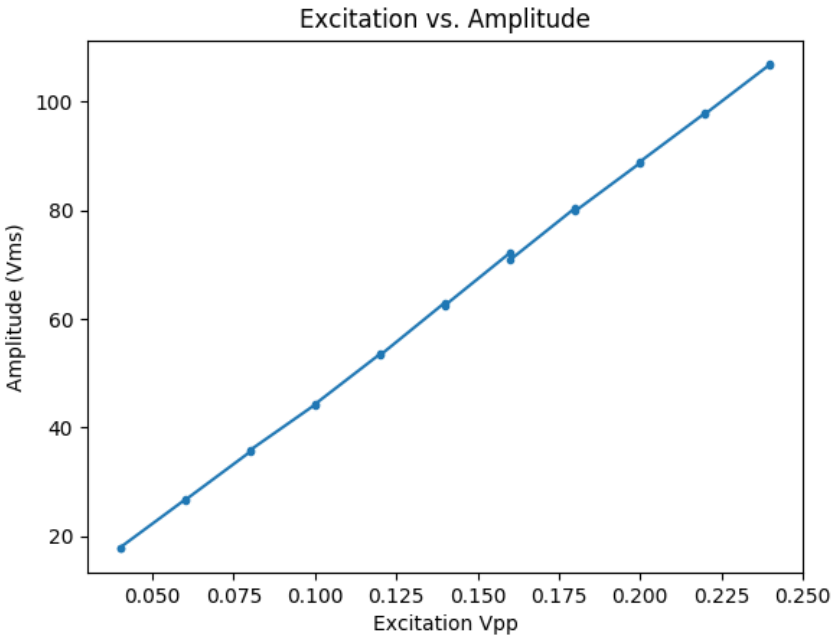

Figure 6: There is a linear relationship between A_V and V_{pp}. The slope of this relationship is used to calculate the transduction factor.

resonance occurred at approximately $14,000Hz$. The chamber is pumped down to vacuum using a cryogenic pump. Beginning at $V_{LF} = 0.04V_{pp}$, an "up" (low ω to high ω) and a "down" (high ω to low ω) sweep is recorded. Additional sweeps are run in $0.02V_{pp}$ increments up to $V_{LF} = 0.24V_{pp}$. Fig. 6 and Fig. 7 express the relationship between amplitude (A_V) and excitation (V_{pp}). β is calculated using ΔA_V and ΔV_{pp}:

$$\beta = \sqrt{\frac{dA_V}{dV_{pp}} \frac{m}{\alpha V_{DC} V_{HF}}}, \tag{10}$$

where α is referred to as the amplification factor: $\alpha = 1.25 \times 10^{12} F^{-1}$.

Following the experimental calculation of β, N_2 is pumped into the chamber at room temperature. Frequency sweeps are conducted around the resonance frequency of the shear mode. The pressure is lowered in logarithmic-like increments. After performing sweeps at vacuum, the same process is

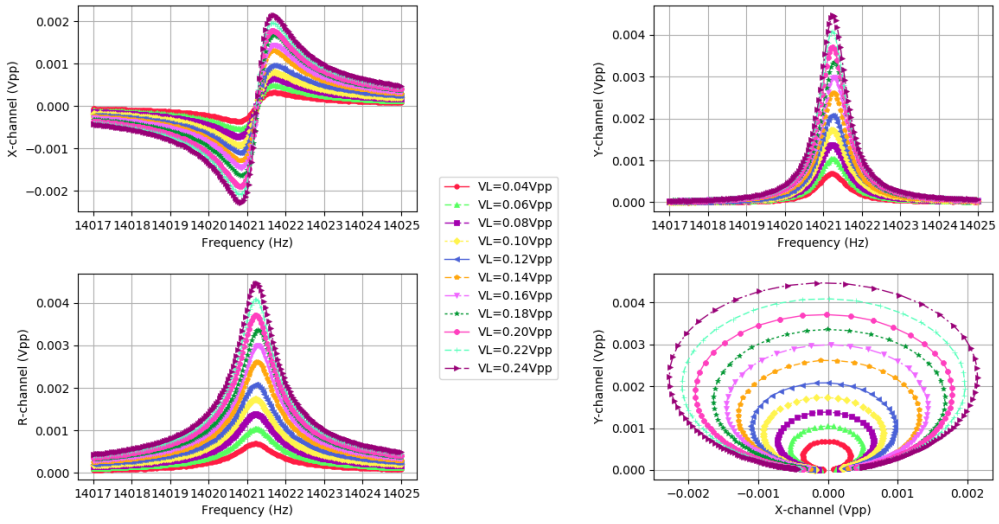

Figure 7: Frequency sweeps with range $V_{LF} = [0.04, .024]$. Increasing the excitation results in a larger amplitude. The top left plot shows the out-of-phase channel. The top right plot shows the in-phase channel. The bottom left plot is the resonance channel. The bottom right plot shows the in-phase vs out-of-phase channels.

repeated using a MEMS device with a substrate. The damping between the two versions of devices is compared.

Results

The experimental calculation of the transduction factor was $\beta = 1.30 \times 10^{-9} \frac{F}{m}$ for a device without a substrate. This is in good agreement with the theoretical value (from Eq. 4) of $\beta = 1.42 \times 10^{-9} \frac{F}{m}$. This suggests that our device had only very small deviations from the intended parameters. In a vacuum, the device had a resonance of $\omega_0 = 14,021 Hz$. Fig. 7 shows that the resonance frequency is independent of excitation. Therefore, any changes in resonance can be directly attributed to pressure.

The width of the resonance curve is equal to the damping coefficient per unit mass:

$$\Delta\omega = \frac{\gamma}{m}. \tag{10}$$

Damping in N_2 was expected to be proportional to $\sqrt{P}$. This would cause the width of resonance to also be proportional to $\sqrt{P}$. However, the width had only small changes at higher pressures (see Fig. 8). The width begins to level at pressures above 100 Torr.

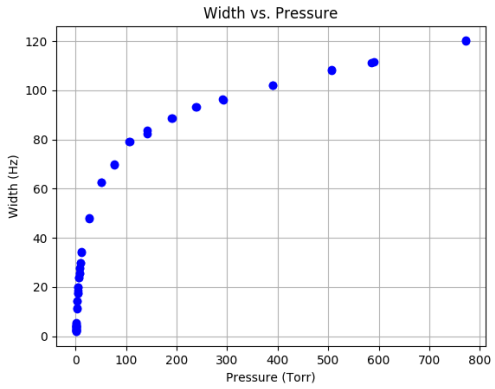

Figure 8: The relationship between the width of the resonance curve and pressure is shown for a MEMS device without a substrate submersed in N_2. The width increases with damping. As pressure increases, the rate of damping decreases.

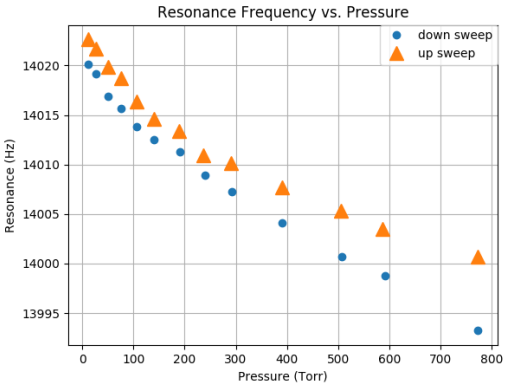

Figure 9: The resonance frequency's dependence on pressure is an indication of the fluid's damping. At lower pressures, the resonance frequency is higher due to less damping force. Each pressure point has a pair of data points, where one is an "up" sweep and the other is a "down" sweep. The down sweeps produce a lower resonance frequency.

Obtaining data from a device with a substrate was unsuccessful due to failures in the measuring apparatus and a power outage. However, a qualitative analysis of damping on MEMS devices with a substrate can be compared to experiments done by Gonzalez [2]. He tested another version of MEMS devices that are constructed of seven layers and six electrodes. Although they

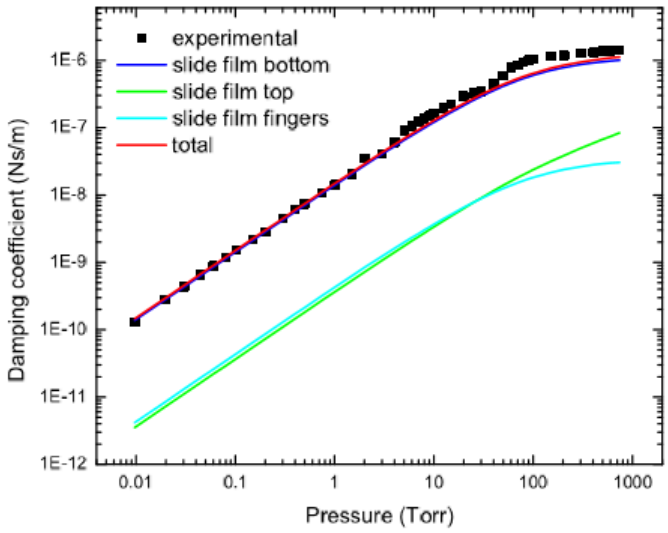

Figure 10: Device with $1.25\mu m$ gap betwen oscillating plate and substrate [2]. There is a linear relationship between pressure and damping until a saturation point.

had different parameters, the relationship between damping and pressure is comparable. Devices with $0.75\mu m$ and $1.25\mu m$ gaps between the plate and substrate were used. Both versions have a linear relationship between pressure and damping until they reach a saturation point in pressure. Recall Eq. 8. No substitution is required for the damping on a device with a substrate. Therefore, the penetration depth is not considered. P only influences K_n. Since $K_n = \frac{\lambda}{d}$ and P is inversely proportional to λ, P is proportional to γ_n. The linear relationship in [2] agrees with the relationship between pressure and damping expected from Eq. 8.

Conclusion

The effects of a substrate on a MEMS device were studied. The substrate acts as a nearby solid boundary that causes damping to be dependent on a small gap rather than the viscous penetration depth of the fluid. N_2 was studied at room temperature to measure the relationship between pressure

and resonance.The pressures ranged from a near vacuum to 1 atmosphere. A MEMS device without a substrate did not have damping proportional to $\sqrt{P}$ as expected. However, Fig. 8 qualitatively resembles a square root relationship. Gonzalez's experiments produced a linear relationship between pressure and damping. The results indicate that a harmonic oscillator without a close boundary experiences damping whose rate changes with pressure, and an oscillator with a substrate experiences damping proportional to pressure in a classical fluid.

Technical difficulties require continued experiments for the three-layered MEMS devices with a substrate. It is expected that these devices will also experience a linear relationship between damping and pressure. Ultimately, similar experiments with MEMS devices can be conducted to compare the damping effects with and without a close boundary in ^4He and ^3He quantum fluids.

Acknowledgments

This work was supported by NSF Grant No. DMR-1461019. I would like to thank everyone involved with the Lee Group at University of Florida. Dr. Yoonseok Lee provided exceptional education and advice throughout this process. His state of the art labs, equipment, teaching methods, and research project allowed me to learn and grow as a physics student by introducing me to a new field of study. He was very dedicated to ensuring that I understood all aspects of my research. Colin Barquist gave me the most guidance and led me through all of the processes of my project. I would like to recognize his patience, for he continuously helped to correct my mistakes and explained new concepts to me over and over again. Wenguang Jiang was especially helpful with giving me the correct computer codes and computer assistance. He helped to drastically improve my Python skills, and took countless time to ensure that my programs were up-to-date. Carlos Banuelos Perez was very helpful running the lab equipment and gave me lots of encouragement. He helped to provide me with a positive learning atmosphere.

I would also like to thank the University of Florida Physics department for holding the Summer 2017 REU program and giving me and other students like myself the opportunity to gain research experience in the sciences. Dr.

Selman Hershfield put in lots of time to coordinate this wonderful program and made me feel especially welcome at the University of Florida. I would also like to recognize John Koptur-Palenchar for his great service to ensure that our living conditions were comfortable and for organizing activities for the REU students.

References

[1] J. Bauer, *Exploration of Electo-mechanical Conversions and Slip-Flow Damping Models In Air and He With a MEMS Comb-drive*, Undergraduate Honors Thesis, University of Florida (2014).

[2] M. Gonzalez, *Development and application of MEMS devices for the study of liquid ^3He*, Ph.D. Disseration Thesis, University of Florida (2012).

[3] M. Gonzalez, P. Zheng, E. Garcell, Y. Lee, and H. B. Chan, *Comb-drive micro-electro-mechanical systems oscillators for low temperature experiments*, Review of Scientific Instruments **84**, 025003 (2013); doi: 10.1063/1.4790196.

[4] P. Zheng, *Study of normal and superfluid ^3He films with micro-electro-mechanical devices*, Ph.D. Dissertation Thesis, University of Florida (2016).